Proceedings on Automation in Medical Engineering
Proc AUTOMED, 2026, Vol. 3, No 1, Article ID 2520, 2 Pages

Infinite Science Publishing

A Twin Robotic CT System Simulation using MuJoCo and gVXR for Medical Applications

L. Freiling[1, *], M. Schaar[1], M. Stille[1, +] and D. Kundrat[1, +]

[1] *Fraunhofer Institution for Individualized and Cell-Based Medical Engineering, Lübeck, Germany*
[+] *These authors contributed equally and share the last position.*
[*] *Corresponding author, email: lukas.freiling@imte.fraunhofer.de*

Abstract: Twin robotic CT systems enable flexible scan trajectories by independently controlling the x-ray source and detector. This work introduces a simulation environment that integrates MuJoCo for robot dynamics and gVXR for x-ray imaging via ROS2, aiming to accelerate trajectory optimization for medical applications. A proof-of-concept scenario with a trajectory on a sphere around the target object demonstrates feasibility. The iterative SART algorithm yields high quality image reconstructions. The framework lays the foundation for exploring novel trajectory strategies, with future work focusing on modeling system uncertainties, optimizing arbitrary scan paths and task-specific image reconstruction.

I. Introduction

A twin robotic CT system, which independently controls x-ray source and detector through separate robotic arms, offers high flexibility in generating specialized scan trajectories for specimens. These systems are promising for medical applications, as they can adjust the geometric relationship between x-ray source and detector on a patient- and task-specific basis, enabling low-dose scanning [1]. Beyond dose reduction, these flexible trajectories can be designed to avoid radiation-sensitive organs or minimize artifacts caused by metal implants, for which sophisticated compensation techniques are currently required [2].

The main challenges in twin robotic CT systems include trajectory planning, system calibration, and 2D/3D image reconstruction [3]. Planning task-specific trajectories is an active area of research [4]. However, this represents even greater challenges in medical context, due to the severely restricted working area and stricter safety regulations. This work presents a simulation environment to facilitate novel trajectory optimization strategies. While simulation tools are independently available for both robotics and x-ray imaging, this work establishes a comprehensive and integrated framework.

II. Methods

This section introduces the modular simulation framework that encompasses the selected independent robot and x-ray simulations. In addition, a proof-of-concept scenario is designed to validate the simulation framework for CT tasks.

II.I Modular Simulation Architecture

For robotic simulation MuJoCo is used [5]. This open-source physics engine is designed for the development of robotics control and mechanics. Fig. 1 shows an exemplary scene of a robotic setup in a virtual operation room. The x-ray simulation is realized using the open-source software

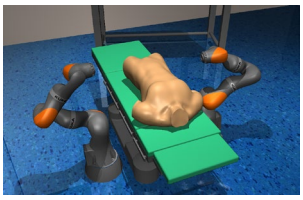

Figure 1: Virtual operating room rendered in MuJoCo.

gVXR [6]. gVXR employs ray tracing techniques for fast image acquisition by sacrificing physical accuracy, e.g. Compton scattering, which is usually obtained using time-consuming Monte Carlo simulations. Both simulations are linked using Robot Operating System 2 (ROS2) [7]. Fig. 2 illustrates the communication architecture. Both the robot and x-ray simulations are initialized through a single file that encodes the scenario parameters. This reduces complexity and ensures consistent definitions of objects in the scenario. The x-ray simulation waits for the robot simulation to submit pose data for the source $\boldsymbol{P_s}$, scanned object $\boldsymbol{P_o}$ and detector $\boldsymbol{P_d}$. To calculate the inverse kinematics the open-source library Mink is used, which interfaces the MuJoCo framework. It receives the joint configurations of source and detector arm $\boldsymbol{q_s}$, $\boldsymbol{q_d}$ and solves the new configurations $\widehat{\boldsymbol{q}}_{\boldsymbol{s}}$, $\widehat{\boldsymbol{q}}_{\boldsymbol{d}}$ based on a target pose of the source $\widehat{\boldsymbol{P}}_{\boldsymbol{s}}$ and detector $\widehat{\boldsymbol{P}}_{\boldsymbol{d}}$. When both robot arms reach a desired pose, the pose information is used to trigger an x-ray projection image $\boldsymbol{I}$. The projections will be used for image reconstruction.

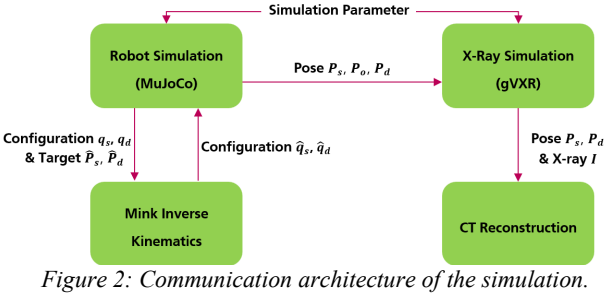

Figure 2: Communication architecture of the simulation.

II.II Example

To verify the functionality of the simulation, a proof-of-concept scenario is created which consists of a trajectory planned on the sphere around the target object with a 300 mm radius. A human skull bone is chosen as the specimen. Fig. 3 shows the trajectory, where the grey sphere indicates the surface on which the end-effectors move. The x-ray source and detector circle 210° (180° + opening angle) longitudinally around the object, with the detector plane always orthogonal to the x-ray source. The latitude angle is modulated using a sine function with an amplitude of 30°. At 399 equidistant poses along the trajectory, x-ray projections are acquired. The accuracy of the inverse kinematics solver is set to 0.1 mm. The robot arm controller considers a position to be reached when the distance between the target and the end-effector is less than 1 mm. The detector resolution is chosen as 640×480 pixels with isotropic pixel size of 0.5 mm. The x-ray source is modeled as a point source with monochromatic x-ray energy of 80 kVp. To reconstruct a volume from the projection images the iterative simultaneous algebraic reconstruction technique (SART) is used [8]. The reconstruction is performed with 10 iterations and a convergence factor of 0.3. The reconstruction grid is 512×512×512 voxels with 0.31 mm isotropic voxel size. Poses of x-ray source and detector end-effectors are used as inputs. To mimic a repeatability of 0.15 mm in robot arms, the input was augmented with normally distributed noise with zero mean and standard deviation of 0.1 mm, with a 0.15 mm cutoff.

Table 1: Translational and rotational error of the end-effector poses from the x-ray source and detector.

Error	μ	σ	max
Source Pos	0.87 mm	0.05 mm	0.98 mm
Source Rot	0.19°	0.03°	0.23°
Detector Pos	0.76 mm	0.07 mm	0.96 mm
Detector Rot	0.20°	0.05°	0.41°

III. Results and Discussion

Table 1 shows mean value, standard deviation and maximum error for both the source and detector end-effector frames, where translation error denotes the Euclidean distance and rotational error is given as axis-angle representation. The maximal translational error for both arms is below 1 mm as expected. The mean error is 0.87 mm for the source and 0.76 mm for the detector. The standard deviation is relatively small compared to the mean error. For the source frame the standard deviation is 0.05 mm and for the detector frame it is 0.07 mm. The rotational mean error for the source is 0.19° with a standard deviation of 0.03° and a maximum value of 0.23°. For the detector frame, the rotational mean error is 0.20° with a standard deviation of 0.05°. The maximum rotational error is nearly doubled compared to the source error, reaching 0.41°. The reconstructed vertical cross-section of the skull is shown in Fig. 3. SART produces clear images in the region of the skull bone with fine details and without streak artefacts. However, due to the limited field of view and the non-optimized trajectory, the jawbone is only partially reconstructed.

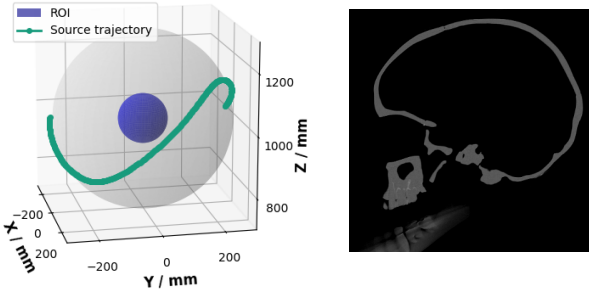

Figure 3: Trajectory of the source end-effector (left) and reconstructed vertical cross-section of the skull (right).

The results demonstrate that the simulation pipeline validates trajectory planning for a twin robotic CT system. Synchronous control of both robot arms was achieved with pose errors remaining within predefined tolerance limits throughout the scanning trajectory. SART produces clear images in the expected regions. However, the current simulation operates under idealized assumptions, including a monochromatic x-ray source and perfect motion control without blur effects. Further investigation is needed to identify limitations of the simulation and assess their impact on reconstruction quality.

IV. Conclusions

This work presents our first steps toward architecture for a twin robotic CT simulation using open-source software MuJoCo and gVXR. Preliminary proof-of-feasibility results with a spheric trajectory are promising and show that a combination of a robot and x-ray imaging simulation provides reasonable reconstructions. Future work will focus on modeling uncertainties in the system, exploration of strategies for arbitrary path planning, and optimization for patient- and task-specific imaging. This also includes object-oriented image reconstruction and regularization strategies to handle imperfections of the scanning process.

Author's Statement

Research funding: This work was partially funded by the European Union-European Regional Development Fund (ERDF), the Federal Government and Land Schleswig Holstein, Project No. 12524009. Conflict of interest: Authors state no conflict of interest.

References

[1] G. Papaioannou et al., *Towards the Performance Characterization of a Robotic Multimodal Diagnostic Imaging System*, J. Imaging, vol. 11, no. 5, p. 147, May 2025.

[2] N. Blum, T. M. Buzug, and M. Stille, *Data-driven metal artifact correction in computed tomography using conditional generative adversarial networks*, ICIFXCT 2022. SPIE, p. 51, Oct. 18, 2022.

[3] G. Herl et al., *RoboCT: The State and Current Challenges of Industrial Twin Robotic CT Systems*, Sensors, vol. 25, no. 10, p. 3076, May 2025.

[4] M. Linde, W. Wiest, A. Trauth, and M. G. R. Sause, *Selecting Feasible Trajectories for Robot-Based X-ray Tomography by Varying Focus-Detector-Distance in Space Restricted Environments*, J Nondestruct Eval, vol. 43, no. 2, May 2024.

[5] E. Todorov, T. Erez, and Y. Tassa, *MuJoCo: A physics engine for model-based control*, 2012 IEEE IROS, pp. 5026–5033, Oct. 2012.

[6] F. P. Vidal and P.-F. Villard, *Development and validation of real-time simulation of X-ray imaging with respiratory motion,* Comput. Med. Imaging Graph., vol. 49, pp. 1–15, Apr. 2016.

[7] S. Macenski, T. Foote, B. Gerkey, C. Lalancette, and W. Woodall, *Robot Operating System 2: Design, architecture, and uses in the wild*, Science Robotics., vol. 7, no. 66, May 2022.

[8] A. Andersen, *Simultaneous Algebraic Reconstruction Technique (SART): A superior implementation of the ART algorithm, Ultrasonic Imaging*, vol. 6, no. 1, pp. 81–94, Jan. 1984.